Interrelating Excess Thermodynamic Functions Using Fusion Properties

Allen R. Hansen
Dept. of Chemical Engineering, University of Illinois, Urbana, IL 61801

Charles A. Eckert
School of Chemical Engineering, Georgia Institute of Technology, Atlanta, GA 30332

A new model that interrelates the liquid-phase excess Gibbs energy, enthalpy and volume, called the GHV model, is developed and discussed. The model is based on the fact that most mixtures are immiscible in solid phases and, therefore, have steep solid-phase boundaries. This single assumption allows the model to be applied potentially to all types of mixtures, including organic, metallic, electrolytic and polymeric solutions. The model, which predicts that excess properties are related to one another through various fusion properties, pure component volumes, and enthalpies of fusion in particular, has been applied to a wide variety of organic and liquid metal mixtures. The results show at least qualitative validity without adjustable parameters and more quantitative ability with "effective" fusion properties. The model is also shown to rationalize some sign, magnitude and shape phenomena.

Introduction

A goal of thermodynamic solution modeling is to simultaneously predict various excess thermodynamic properties for a wide variety of compounds and their mixtures. A model's ability to achieve this goal is a stringent test of its representation of underlying physics and general applicability. A new model developed in this work interrelates excess Gibbs energies, enthalpies and volumes, called the GHV (pronounced 'give') model. Such a model should be extremely useful in estimating thermodynamic properties that are unavailable and in reducing the number of experiments that need to be performed. Also, modeling efforts have concentrated extensively on the excess Gibbs energy, leaving little attention for other properties. The model developed here advances the potential for further emphasis on the modeling of derivative properties such as enthalpies and volumes, which seem to be more comprehensible physically.

The GHV model is appealing because it is derived in a fairly rigorous, fundamental manner, utilizing a few assumptions. The model has wide applicability since it is based on a feature of solid–liquid-phase diagrams that is very common in all types of mixtures, including organic, metallic, electrolytic and polymeric solutions. The model predicts that fusion properties, which contain both structural and thermodynamic information, are important in interrelating the excess properties, and it helps rationalize the factors affecting sign, magnitude and shape phenomena.

Model Development

The model to be developed here is actually an extension of a recent model by Hansen and Eckert (1989) that interrelates excess volumes and enthalpies. That relationship and the GHV model developed here are based on the fact that most mixtures are immiscible in solid phases. Figure 1 illustrates some typical phase diagrams that range from fairly ideal, solid solution and simple eutectic types of mixtures (Figures 1a and 1b, respectively) to highly nonideal, compound-forming and liquid-liquid immiscibility systems (Figures 1c and 1d, respectively). It turns out, however, that solid solution systems, which exhibit complete miscibility in the solid phase, are somewhat rare. Most mixtures fall into the other categories that have immiscible solid phases and, therefore, steep solid-phase boundaries. It

Correspondence concerning this article should be addressed to C. A. Eckert.
Present address of A. R. Hansen: Mobil Research and Development Corp., Paulsboro Research Laboratory, Paulsboro, NJ 08066.

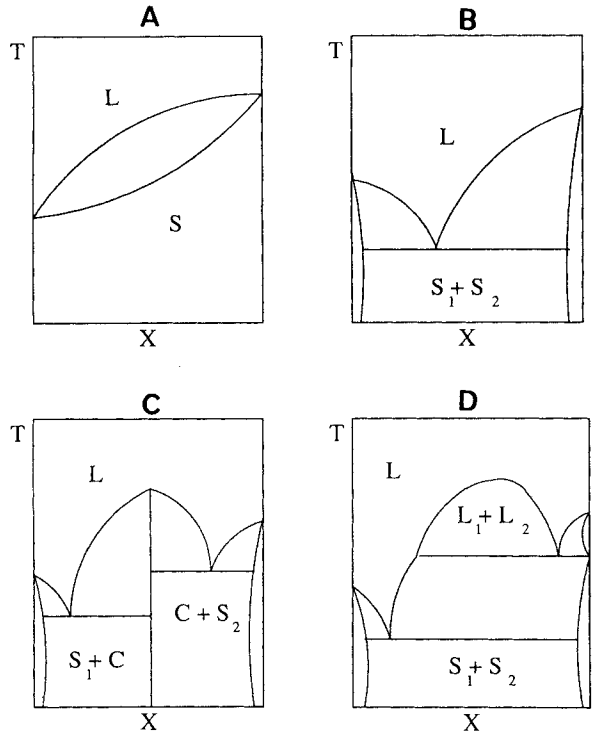

Figure 1. Common solid-liquid phase diagrams.
a. Solid-solution forming system
b. Simple eutectic system
c. Compound-forming system
d. Liquid-liquid immiscibility systems

is this physical feature, which is common to all types of solutions, along with the traditional thermodynamic relationships, that will be exploited to develop our model.

The derivation involves writing the thermodynamic relationships along the lines of solid-liquid equilibrium (SLE). First, the chemical potentials of species 2 in the liquid and solid phases may be equated along a line of SLE where the composition and temperature are varied at constant pressure.

$$d(\mu_2^L/T)_{\text{SLE}} = d(\mu_2^S/T)_{\text{SLE}} \tag{1}$$

$$[\partial(\mu_2^L/T)\partial T]_{x,P}dT + (\partial(\mu_2^L/T)/\partial x_1^L)_{T,P}dx_1^L = [\partial(\mu_2^S/T)/\partial T]_{x,P}dT + [\partial(\mu_2^S/T)/\partial x_1^S]_{T,P}dx_1^S \tag{2}$$

$$-(\bar{h}_2^L/T^2)dT + R[(-1/x_2^L) + (\partial\ln\gamma_2^L/\partial x_1^L)_{T,P}]dx_1^L = -(\bar{h}_2^S/T^2)dT + R[(-1/x_2^S) + (\partial\ln\gamma_2^S/\partial x_1^S)_{T,P}]dx_1^S \tag{3}$$

In the region of dilute species 1, dx_1^S is much smaller than dx_1^L, and the dT terms when the solid-phase boundaries are very steep. This allows the last term in Eq. 3 to be ignored. Also, since $(\partial n\gamma_2^L/\partial x_1^L)_{T,P}$ is very small in the region of very dilute species 1, the following equation is obtained for the slope of liquidus line in the region where x_2 approaches 1:

$$RT^2(dx_1^L/dT)_{\text{SLE}} = -x_2^L(\bar{h}_2^L - \bar{h}_2^S) = -x_2^L[\Delta h_{f2}^\circ + \Delta C_{Pf2}^\circ(T - T_{M2}) + \bar{h}_2^{E,L} - \bar{h}_2^{E,S}] \tag{4}$$

This relationship for the nondilute component (species 2) has been derived and described by a number of researchers (see, for example, Denbigh, 1981; Prausnitz et al., 1986). However, the relationships for the dilute component (species 1) have not as yet been developed adequately. An equation similar to Eq. 3 may be written for species 1 as well.

$$-(\bar{h}_1^L/T^2)dT + R[(1/x_1^L) + (\partial\ln\gamma_1^L/\partial x_1^L)_{T,P}]dx_1^L = -(\bar{h}_1^S/T^2)dT + R[(1/x_1^S) + (\partial\ln\gamma_1^S/\partial x_1^S)_{T,P}]dx_1^S \tag{5}$$

Since we are interested in the region that is very dilute in species 1, the $1/x_1$ terms of Eq. 5 are extremely large, and the last term cannot merely be ignored. This is where the problem arises when dealing with the very dilute component. In the very dilute region, however, we may assume that the slopes of the liquidus and solidus lines are linear such that $(dx_1^L/dT)_{\text{SLE}} = (x_1^L - 0)/(T - T_{M2})$ and $(dx_1^S/dT)_{\text{SLE}} = (x_1^S - 0)/(T - T_{M2})$. Combining these gives the relationship $(dx_1^L/dx_1^S)_{\text{SLE}} = x_1^L/x_1^S$ in the region where x_2 approaches 1. Therefore, Eq. 5 becomes,

$$-(\bar{h}_1^L/T^2)dT + R(\partial\ln\gamma_1^L/\partial x_1^L)_{T,P}dx_1^L = -(\bar{h}_1^S/T^2)dT + R(\partial\ln\gamma_1^S/\partial x_1^S)_{T,P}(x_1^S/x_1^L)dx_1^L \tag{6}$$

The $1/x$ terms have not been ignored, but have cancelled out. Since (x_1^S/x_1^L) is very small for a mixture with immiscible solid phases, the last term in Eq. 6 may be ignored, as was done in the equations for species 2.

$$RT^2(dx_1^L/dT)_{\text{SLE}} = (\bar{h}_1^L - \bar{h}_1^S)/(\partial\ln\gamma_1^L/\partial x_1^L)_{T,P} = [\Delta h_{f1}^\circ + \Delta C_{Pf1}^\circ(T - T_{M1}) + \bar{h}_1^{E,L} - \bar{h}_1^{E,S}]/(\partial\ln\gamma_1^L/\partial x_1^L)_{T,P} \tag{7}$$

Equations 4 and 7 can now be set equal in the region of very dilute species 1 along the lines of SLE at constant pressure.

$$[\Delta h_{f1}^\circ + \Delta C_{Pf1}^\circ(T - T_{M1}) + \bar{h}_1^{E,L} - \bar{h}_1^{E,S}]/(\partial\ln\gamma_1^L/\partial x_1^L)_{T,P} = -x_2^L[\Delta h_{f2}^\circ + \Delta C_{Pf2}^\circ(T - T_{M2}) + \bar{h}_2^{E,L} - \bar{h}_2^{E,S}] \tag{8}$$

The goal is to derive a liquid-phase relationship. Therefore, the solid-phase partial molar excess enthalpies must be eliminated. Even though $\bar{h}_2^{E,S}$ could be ignored, $\bar{h}_1^{E,S}$ cannot and should not be ignored. These undesirable properties can be eliminated, however, by taking liquid-phase composition derivatives of both sides of Eq. 8, along the line of SLE, for which Eq. 8 applies. Extending the resulting equation to infinite dilution of species 1 gives,

$$(\Delta h^{\circ}_{f1} + \bar{h}^{E,L\infty}_1 - \bar{h}^{E,S\infty}_1)/(\partial \ln\gamma^L_1/\partial x^L_1)^{\infty}_{T,P}$$

$$= \frac{-(\partial \ln\gamma^L_1/\partial x^L_1)^{\infty}_{T,P}[\Delta h^{\circ}_{f2} - (dT/dx^L_1)^{\infty}_{\mathrm{SLE}}\Delta C^{\circ}_{Pf2}] + (\partial \bar{h}^{E,L}_1/\partial x^L_1)^{\infty}_{T,P} - (\partial \bar{h}^{E,S}_1/\partial x^S_1)^{\infty}_{T,P}(dx^S_1/dx^L_1) + (dT/dx^L_1)^{\infty}_{\mathrm{SLE}}[\Delta C^{\circ}_{Pf1} + \Delta_f(\partial \bar{h}^E_1/\partial T)^{\infty}_{x,P}]}{[(\partial^2 \ln\gamma^L_1/\partial x^{L2}_1)^{\infty}_{T,P} - (dT/dx^L_1)^{\infty}_{\mathrm{SLE}}(\partial \bar{h}^{E,L}_1/\partial x^L_1)^{\infty}_{T,P}/RT^2_{M2}]}$$

at T_{M2} (9)

where

$$\Delta_f(\partial \bar{h}^E_1/\partial T)^{\infty}_{x,P} = (\partial \bar{h}^{E,L}_1/\partial T)^{\infty}_{x,P} - (\partial \bar{h}^{E,S}_1/\partial T)^{\infty}_{x,P}.$$

The Gibbs-Duhem equation was utilized in developing Eq. 9 to show that $(\partial \bar{h}^{E,L}_2/\partial x^L_1)^{\infty}_{T,P} = (\partial \bar{h}^{E,S}_2/\partial x^S_1)^{\infty}_{T,P} = 0$ at $x_2 = 1$. Also, $\bar{h}^{E,L}_2 = \bar{h}^{E,S}_2 = 0$ at $x_2 = 1$. Equation 9 may be simplified further by ignoring the term $(\partial \bar{h}^{E,S}_1/\partial x^S_1)^{\infty}_{T,P}(dx^S_1/dx^L_1)$ (again utilizing the assumption of immiscible solid phases) and by recognizing that $(dx^L_1/dT)^{\infty}_{\mathrm{SLE}} = -\Delta h^{\circ}_{f2}/RT^2$ as taken from Eq. 3. Equation 8 may also be extended to infinite dilution of species 1.

$$[\Delta h^{\circ}_{f1} + \Delta C^{\circ}_{Pf1}(T_{M2} - T_{M1}) + \bar{h}^{E,L\infty}_1 - \bar{h}^{E,S\infty}_1]/(\partial \ln\gamma^L_1/\partial x^L_1)^{\infty}_{T,P} = -\Delta h^{\circ}_{f2} \quad \text{at } T_{M2} \quad (10)$$

Equations 9 and 10 are now combined to give the final relationship between γ^L_1 and $\bar{h}^{E,L}_1$:

$$(\partial \ln\gamma^L_1/\partial x^L_1)^{\infty}_{T,P}[1 + (RT^2_{M2}/\Delta h^{\circ 2}_{f2})\Delta C^{\circ}_{Pf2}] - (\partial^2 \ln\gamma^L_1/\partial x^{L2}_1)^{\infty}_{T,P} = (2/\Delta h^{\circ}_{f2})(\partial \bar{h}^{E,L}_1/\partial x^L_1)^{\infty}_{T,P} - (RT^2_{M2}/\Delta h^{\circ 2}_{f2})[\Delta C^{\circ}_{Pf1} + \Delta_f(\partial \bar{h}^E_1/\partial T)^{\infty}_{x,P}] \quad \text{at } T_{M2} \quad (11)$$

At the other end of the composition range, a similar equation may be derived for species 2.

$$(\partial \ln\gamma^L_2/\partial x^L_1)^{\infty}_{T,P}[1 + (RT^2_{M1}/\Delta h^{\circ 2}_{f1})\Delta C^{\circ}_{Pf1}] + (\partial^2 \ln\gamma^L_2/\partial x^{L2}_1)^{\infty}_{T,P} = (2/\Delta h^{\circ}_{f1})(\partial \bar{h}^{E,L}_2/\partial x^L_1)^{\infty}_{T,P} + (RT^2_{M1}/\Delta h^{\circ 2}_{f1})[\Delta C^{\circ}_{Pf2} + \Delta_f(\partial \bar{h}^E_2/\partial T)^{\infty}_{x,P}] \quad \text{at } T_{M2} \quad (12)$$

Equations 11 and 12, which interrelate excess Gibbs energies and enthalpies, were derived by determining property changes along the lines of SLE where the composition and temperature were varied. However, if lines of changing composition and pressure (at constant temperature) are utilized, the following equations, which interrelate partial molar excess volumes and activity coefficients, are obtained:

$$(\partial \ln\gamma^L_1/\partial x^L_1)^{\infty}_{T,P}[1 - (RT_{M2}/\Delta v^{\circ 2}_{f2})\Delta \beta^{\circ}_{f2}] - (\partial^2 \ln\gamma^L_1/\partial x^{L2}_1)^{\infty}_{T,P} = (2/\Delta v^{\circ}_{f2})(\partial \bar{v}^{E,L}_1/\partial x^L_1)^{\infty}_{T,P} + (RT_{M2}/\Delta v^{\circ 2}_{f2})[\Delta \beta^{\circ}_{f1} + \Delta_f(\partial \bar{v}^E_1/\partial P)^{\infty}_{x,P}] \quad \text{at } T_{M2} \quad (13)$$

$$(\partial \ln\gamma^L_2/\partial x^L_1)^{\infty}_{T,P}[1 - (RT_{M1}/\Delta v^{\circ 2}_{f1})\Delta \beta^{\circ}_{f1}] + (\partial^2 \ln\gamma^L_2/\partial x^{L2}_1)^{\infty}_{T,P} = (2/\Delta v^{\circ}_{f1})(\partial \bar{v}^{E,L}_2/\partial x^L_1)^{\infty}_{T,P} - (RT_{M1}/\Delta v^{\circ 2}_{f1})[\Delta \beta^{\circ}_{f2} + \Delta_f(\partial \bar{v}^E_2/\partial P)^{\infty}_{x,P}] \quad \text{at } T_{M2} \quad (14)$$

where $\Delta \beta^{\circ}_{fi} = (\partial v^L_i/\partial P)_T - (\partial v^S_i/\partial P)_T$ and $\Delta_f(\partial \bar{v}^E_i/\partial P)^{\infty}_{x,P} = (\partial \bar{v}^{E,L}_i/\partial P)^{\infty}_{x,P} - (\partial \bar{v}^{ES}_i/\partial P)^{\infty}_{x,P}$. Equations 11 through 14 constitute the GHV model that interrelates excess Gibbs energies, enthalpies, and volumes. These equations were derived with the single assumption that the mixture exhibits immiscibility in the solid phases such that $dx^S_1/dx^L_1 \approx 0$. Therefore, the model equations may not be applicable to mixtures, for which this assumption is not acceptable, such as for the systems with significant solid solubilities, and should not be utilized automatically.

The significance of fusion properties has some intuitive appeal since fusion or melting is just a change in structure. Associated with that change in the structure are energy and density changes as well. There are comparable local structural changes for mixtures. Therefore, it is reasonable to expect fusion properties to contain information that could be useful in helping to rationalize solution behavior. In the following sections, the practical potential of the ideas developed here shall be evaluated.

Model Results and Discussion

It is difficult to test the GHV model equations directly using experimental data since they involve composition derivatives of excess properties at infinite dilution. Also, the model equations were derived at the melting points of the species, which are generally far removed from 25°C, where most organic data are available and fusion properties other than Δv°_f and Δh°_f are generally not available. Despite these problems, the model was tested in a simple manner by first applying the equations at the experimental temperatures. Second, fusion properties other than Δv°_f and Δh°_f were assumed to be negligible. As will be discussed subsequently, this assumption is very good for the relationships between the excess Gibbs energy and enthalpy, but very poor for the relationships involving the excess volume. Finally, a two-parameter Redlich-Kister type of expression was chosen to represent the excess properties across the entire composition range,

$$\theta^E = x_1 x_2 [A_\theta + B_\theta (x_1 - x_2)] \quad (15)$$

where θ^E represents g^E, h^E, or v^E. A Redlich-Kister form is clearly not correct, particularly for mixtures that exhibit specific chemical interactions, but is useful for its simplicity and versatility.

Table 1. Effective Fusion Properties

Ref. No.	Compound	Δv_{EFF} $10^{-9}m^3/mol$	Δh_{EFF} J/mol	$\Delta C_{P,EFF}$ J/mol•K	$\Delta\beta_{EFF}$ $10^{-9}m^3/mol\cdot bar$
1	Acetone	2,871	7,030	202.7	−2.26
2	Benzene	1,679	4,441	40.3	−0.66
3	1-Butanol	63,333	17,070	245.8	−3.39
4	Carbon Disulfide	4,288	5,316	−48.1	1.23
5	Carbon Tetrachloride	1,074	4,726	15.4	−0.79
6	Chlorobenzene	Large	4,694	−6.54	−0.60
7	Chloroform	4,569	7,622	−12.3	1.24
8	Cyclohexane	3,832	4,171	6.4	0.56
9	1,2 Dichloroethane	3,944	6,988	19.4	0.15
10	1,4 Dioxane	4,670	12,356	69.8	−0.14
11	Ethanol	Large	Large	318.0	−4.59
12	*n*-Heptane	2,695	4,565	−1.15	−0.15
13	*n*-Hexane	2,945	4,714	−4.9	−0.18
14	Methanol	635	18,523	517.4	−7.59
15	Methylcyclohexane	−626	4,941	−7.65	−0.64
16	*n*-Octane	4,100	6,386	−71.2	1.04
17	Toluene	2,755	5,708	1.23	−0.21
18	*p*-Xylene	Large	5,724	−3.72	−0.33

When the appropriate derivatives of the Redlich-Kister relationships are performed and extended to infinite dilution, the GHV model equations may be used to estimate the parameters for two of the excess properties from the knowledge of A_θ and B_θ for the third excess property. This was done for a number of diverse organic and liquid metal solutions, and the results for the prediction of equimolar excess Gibbs energies from excess enthalpy data are shown in Table 2 and Figures 2a and 2b. The prediction of excess Gibbs energies and enthalpies from excess volume data are also given in Table 2 and shown in Figures 3 and 4. The literature values for the volumes and enthalpies of fusion used in the predictions are presented in Table 3. The reverse predictions could be performed equally well, but are not shown to avoid redundancy.

The excess Gibbs energies predicted from excess enthalpy data are generally fairly good, despite the conditions that were imposed on the GHV model and the highly diverse species and mixtures included in the database. The mixtures that are represented least well are generally methanol and ethanol solutions, which are likely to be the most sensitive to the assumptions regarding temperature extrapolation of the model and temperature dependencies of the excess properties. Also, the experimental excess Gibbs energy data are likely to have somewhat larger errors, as compared to experimental excess volume and enthalpy data, since they were determined from vapor-liquid equilibrium data fit to the Wilson equation (Gmehling et al., 1980). The predictions for the liquid metal solutions are also fairly good and exemplify the versatility and wide applicability of the GHV model. As mentioned earlier, ignoring ΔC_{Pf}° and $\Delta_f(\partial\bar{h}_1^E/\partial T)_{x,P}^{\infty}$ in Eqs. 11 and 12 is not a bad assumption since typical magnitudes of the terms involving these quantities are relatively small compared to the heat of fusion terms.

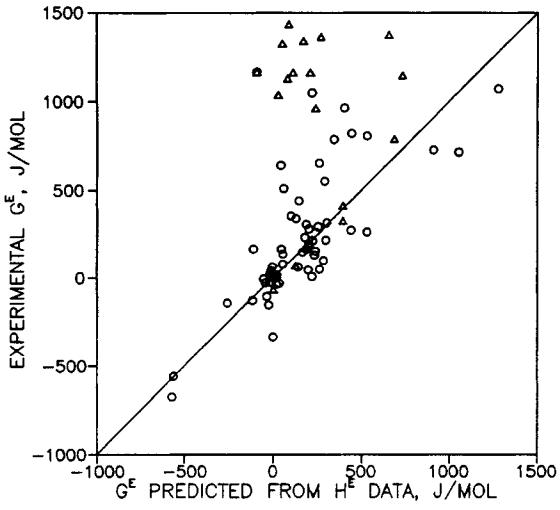

a. Organic solutions, Δ indicates alcohol mixtures

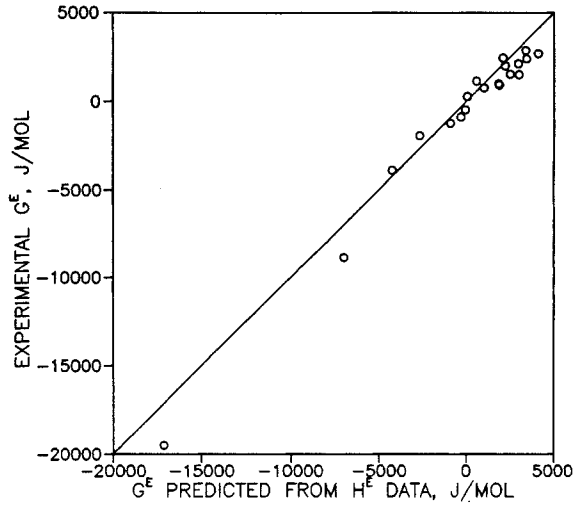

b. Liquid metal solutions

Figure 2. Equimolar excess Gibbs energies predicted from excess enthalpy data using literature values of Δh_f°.

Table 2. Comparison between Calculated Excess Properties and Experimental Data for Equimolar Mixtures at 25°C

Mixtures* Ref. Nos.	Using Literature Fusion Properties J/mol g^E	g^E Calculated from h^E	v^E	h^E	Using Effective Fusion Properties J/mol g^E	g^E Calculated from h^E	v^E	h^E	Experimental** 10^{-9} m³/mol J/mol g^E	h^E	v^E
Organic Mixtures											
1,2	45	−24	−72	375	405	185	641	153	−69		
1,4	404	620	1,270	1,017	931	612	964	750	1,016		
1,5	292	−64	−200	524	447	52	553	281	−100		
1,7	−561	23	−121	−359	−17	−657	−558	−1,916	−94		
1,8	1,278	590	964	1,085	905	949	1,070	1,632	1,147		
1,14	396	−413	−687	371	359	189	413	727	−399		
1,17	101	−99	−247	353	290	−107	355	247	−186		
2,5	55	4	2	146	253	429	81	116	6		
2,6	−1	6	25	85	137	212	65	−6	24		
2,7	−112	39	152	−115	−151	−435	−127	−409	156		
2,8	442	229	487	442	372	525	275	806	655		
2,9	23	80	291	92	166	370	17	77	256		
2,10	−9	3	20	110	37	−78	44	−33	−67		
2,11	31	−154	−174	1,128	1,126	1,497	1,038	814	34[1]		
2,12	221	150	693	433	433	839	1,050	911	586		
2,13	129	105	488	357	337	601	340	608	415		
2,14	−89	−135	−135	1,224	1,214	−2,162	1,165	696	−7		
2,15	222	276	807	389	334	737	217	790	574		
2,16	238	170	717	374	302	757	157	977	741		
2,17	20	26	67	88	172	291	−36	68	44		
2,18	37	42	188	119	143	253	−28	168	208		
3,5	687	42	−242	902	863	1,111	790	395	−19[2]		
3,8	732	199	203	1,088	1,100	1,230	1,146	625	405		
3,11	23	15	25	51	2	−414	21	48	12		
3,12	81	59	504	1,056	1,094	1,259	1,130	600	208[3]		
3,14	128	233	272	114	95	55	73	145	77		
3,15	241	190	509	1,015	963	1,114	963	557	238		
4,8	297	311	463	189	342	666	220	437	522		
4,10	260	475	1,570	549	657	1,260	654	792	776		
4,17	187	210	438	186	102	167	167	349	337		
5,6	47	−64	−154	67	111	203	168	84	−158		
5,8	143	79	94	135	52	−71	64	165	166		
5,9	303	141	261	280	161	391	317	632	327		
5,10	−108	−126	−101	83	−5	−100	169	−246	−279		
5,12	233	97	169	209	232	389	135	372	217		
5,13	205	25	12	177	155	252	184	318	46		
5,14	169	−245	−312	1,283	1,302	−2,811	1,341	242	−35		
5,16	284	137	227	56	−21	182	102	377	318		
5,17	−14	−20	−20	20	149	301	24	−17	−43		
5,18	−33	−4	71	−14	62	97	−105	−74	78		
6,8	532	178	214	390	471	851	265	706	372		
6,12	148	−82	−309	379	143	291	441	701	−237		
6,17	−40	−41	−122	−70	78	197	−27	−124	−90		
6,18	−23	−136	−72	−84	0	45	−153	−118	−76		
7,10	−570	−8	94	−624	−518	−1,635	−675	−1,991	−213[4]		
7,12	203	708	766	292	199	742	282	805	503		
7,13	188	100	476	295	56	297	307	764	335		
7,14	−1,042	−370	−446	820	893	−1,326	782	−262	−137		
7,17	−255	26	78	−321	−244	−519	−142	−719	58		
8,9	910	396	1,107	687	793	2,020	727	1,614	966		
8,10	1,055	484	786	812	863	1,426	714	1,614	966		
8,11	653	389	629	1,311	1,269	587	1,374	710	602		
8,12	221	154	104	146	168	278	10	244	302		
8,13	200	84	10	123	55	89	48	143	219		
8,15	−1	8	17	2	−106	−192	31	18	13		
8,16	262	198	162	−77	67	474	52	261	381[5]		
8,17	253	288	391	186	437	741	295	351	583		

Table 2 (continued)

Mixtures* Ref. Nos.	Using Literature Fusion Properties J/mol g^E	h^E	v^E	Using Effective Fusion Properties J/mol g^E	h^E	v^E	Experimental** 10^{-9} m³/mol J/mol g^E	h^E	v^E
	Calculated from			Calculated from					
Organic Mixtures (Continued)									
9,12	445	288	1,391	844	644	1,455	822	1,999	888
9,17	−51	79	235	−22	119	268	−5	−126	179
10,12	345	450	2,364	808	917	1,939	787	1,694	1,248
10,14	396	−555	−995	300	366	627	328	980	−375
10,17	55	−8	−25	169	34	−151	139	185	−15
11,12	112	253	899	1,267	1,276	716	1,163	672	514
11,13	50	37	652	1,340	1,298	768	1,326	619	472[1]
11,14	4	18	24	38	124	92	−65	5	9
11,15	267	354	849	1,296	1,332	944	1,363	726	445
11,16	88	371	902	1,413	1,430	762	1,435	730	552
11,17	209	−113	−147	1,115	1,102	1,274	1,163	739	−39
12,13	−5	−8	−45	−31	45	110	−26	−25	−28[6]
12,15	12	−5	−37	−5	129	270	1	36	−21
12,17	180	58	214	258	168	342	235	556	137
13,15	4	−53	−247	−28	68	179	8	11	−162
13,16	1	−21	−122	−269	−317	−64	−335	4	−84[6]
13,17	167	−29	−40	295	48	86	151	600	−32
13,18	61	−45	−263	166	−12	17	511	353	−239[7]
15,17	201	267	727	255	145	386	199	540	388
17,18	6	6	21	4	74	180	−40	19	18
Alloys									
19,27	3,379	1,653	2,339				2,858	4,139	166[8]
21,23†	−2,669	1,227	1,084				−1,921	−1,777	308[9]
21,24†	−901	10	−199				−1,226	−1,065	53[9]
21,27†	61	−434	−290				276	104	−140[9]
21,26†		606	−1,908				−4,690	−4,427	594[9]
21,28†	4,094	169	1				2,678	4,600	190[8]
22,23	1,846	1,717	1,235				992	1,442	126[9]
22,24	2,948	1,805	1,713				2,109	2,706	159[9]
22,27	1,879	2,962	2,944				920	1,842	238[9]
22,26	2,488	1,578	1,459				1,527	2,306	140[9]
22,28	2,202	624	509				2,000	2,118	66[9]
23,24		797					603		86[9]
23,20†	−4,230	−4,870	−18,219				−3,883	−3,175	249[10]
23,27	−298	−384	−284				−874	−200	−29[9]
23,26	1,010	2,999	1,524				762	558	201[9]
23,28	3,426	907	954				2,393	3,272	71[9]
24,20	−49	−527	−2,659				−469	−53	76[10]
27,26	573	4,382	4,179				1,138	694	314[9]
27,28	2,992	2,581	2,745				1,498	3,180	195[9]
25,21	−17,132	−17,779	−19,500				−19,800	−18,592	−407[9]
25,24	−6,979	−11,290	−12,932				−8,828	−9,274	−595[9]
24,27	2,077						2,439	1,389[9]	

*Reference numbers refer to the compounds as numbered in Tables 1 and 3.
**Excess Gibbs energy data taken from Gmehling et al. (1980).
Excess enthalpy data taken from Christensen et al. (1984).
Excess volume data taken from Handa and Benson (1979) except as noted:

1. Marsh and Burfitt (1975)
2. Lepori and Matteoli (1986)
3. Treszczanowicz and Benson (1977)
4. Nigam et al. (1972)
5. Sanchez-Pajares and Delgado (1979)
6. Goates et al. (1981)
7. Rodgriguez-Nunez et al. (1985)
8. Hansen et al. (1989)
9. Lira (1986)
10. Hansen et al. (1990).

†Mixtures for which only a one-parameter Redlich-Kister relationship was used.

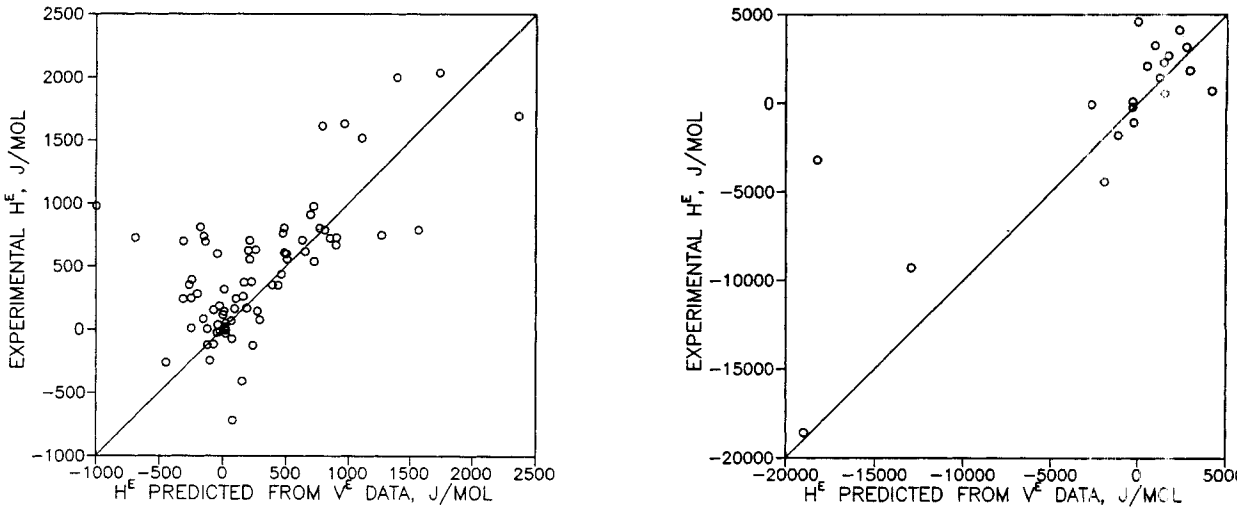

a. Organic solutions *b. Liquid metal solutions*

Figure 3. Equimolar excess enthalpies predicted from excess volume data using literature values of Δv_f° and Δh_f°.

The excess enthalpies predicted from excess volume data (as shown in Figure 3a) show only qualitative agreement. The results here are not as good as the predictions from excess enthalpy data for a number of reasons. First, and most importantly, typical values for the $\Delta\beta_{fi}^\circ$ terms that were ignored in Eqs. 13 and 14 are usually too large to be ignored. Second, excess volume curves are often very asymmetric or even 'S'-shaped; due to the composition derivatives involved, the GHV model equations are somewhat sensitive to such complicated shapes. Third, the volume changes on fusion were determined indirectly from literature values of $(dT_{Mi}/dP)_{SLE} = (T_{Mi}\Delta v_{fi}^\circ/\Delta h_{fi}^\circ)$ (Babb, 1963; Hamann, 1957) and Δh_{fi}° (Weast and Astle, 1980). Therefore, the volume changes on fusion are less accurate than enthalpies of fusion. Again, the results for liquid metal solutions (shown in Figure 3b) are fairly good.

The fact that the model is capable of predicting the proper magnitudes of the excess enthalpies for both organic and metallic solutions is remarkable since excess volumes of metallic mixtures are generally two to four times smaller than typical organic excess volumes. Also, excess enthalpies for metallic solutions are two to four times larger than typical organic excess enthalpies. However, since volume changes on fusion are an order of magnitude smaller for metals, and excess enthalpies are related to excess volumes by the inverse of Δv_{fi}°, the proper magnitudes of the excess properties are preserved. Therefore, the GHV model has provided some insight into the factors which make metallic solutions so regular (i.e., small excess volumes and entropies).

The excess Gibbs energies for organic solutions, predicted from excess volume data (shown in Figure 4a), are very poor. The reasons for this have been described previously. As usual, the predictions for metallic solutions are much better.

The reasons why liquid metal solutions are usually handled better can be rationalized by evaluating the factors that affect

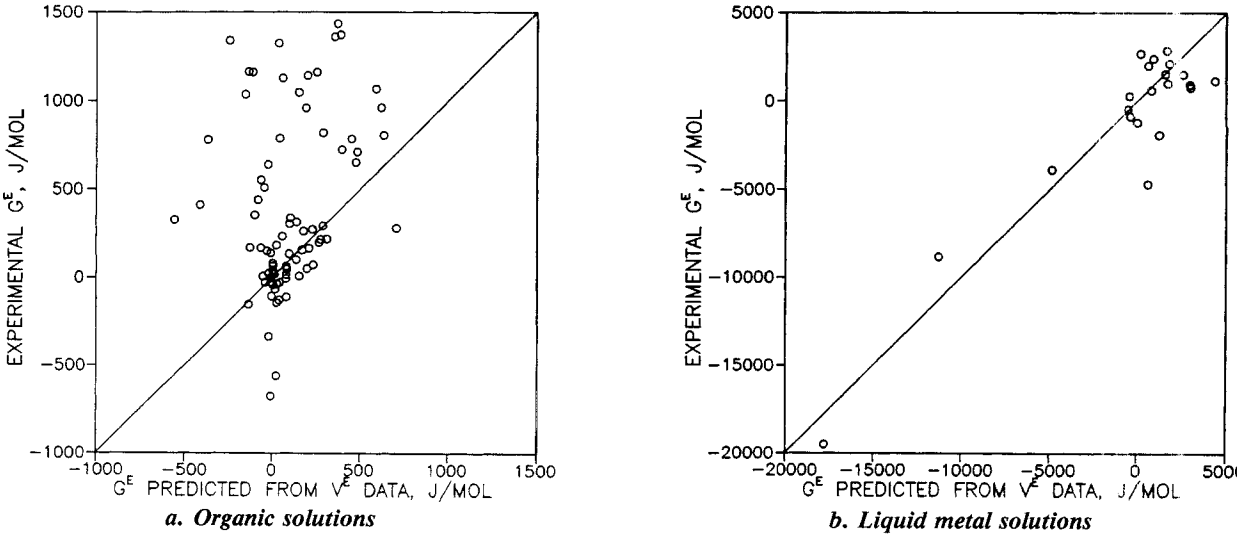

a. Organic solutions *b. Liquid metal solutions*

Figure 4. Equimolar excess Gibbs energies predicted from excess volume data using literature values of Δv_f° and Δh_f°.

Table 3. Literatures values for Δv_f° and Δh_f°

Ref. No.	Compound	Δv_f° $10^{-9}m^3/mol$*	Δh_f° J/mol**
1	Acetone	4,514	5,684
2	Benzene	10,617	9,938
3	1-Butanol	7,485	9,267
4	Carbon Disulfide	3,545	4,388
5	Carbon Tetrachloride	5,292	3,276
6	Chlorobenzene	7,239	9,598
7	Chloroform	6,950	8,799
8	Cyclohexane	5,078	2,625
9	1,2 Dichloroethane	7,158	8,740
10	1,4 Dioxane	4,358	10,499
11	Ethanol	2,937	5,014
12	*n*-Heptane	7,990	14,134
13	*n*-Hexane	8,896	13,051
14	Methanol	1,110	3,173
15	Methylcyclohexane	3,264	6,737
16	*b*-Octane	14,515	20,611
17	Toluene	4,776	6,609
18	*p*-Xylene	20,536	16,778
19	Aluminum	733	10,669
20	Antimony	−129	19,958
21	Bismuth	−687	10,481
22	Cadmium	566	6,109
23	Indium	397	3,268
24	Lead	659	5,121
25	Magnesium	439	9,038
26	Thallium	488	4,310
27	Tin	371	7,197
28	Zinc	463	6,674

*Volume changes on fusion were calculated using Δh_f° and pure component $(dT/dP)_{SLE}$ information from Babb (1963) and Hamann (1957).
**Heat of fusion data were taken from Weast and Astle (1980).

the model's performance. First, the excess properties for metallic solutions generally do not exhibit the complex shapes found for organic solutions, since metal atoms have simple, spherical symmetry and do not differ very much in molar volume. This alleviates many of the problems associated with the imposed Redlich-Kister relationship and the derivatives involved in the model. Also, the fusion properties other than Δv_{fi}° and Δh_{fi}° are usually less significant for metals and, therefore, can be ignored with less trouble.

The model potentially can explain other phenomena as well. For example, excess volumes occasionally exhibit anomalous sign behavior, while excess Gibbs energies and enthalpies are usually of the same sign. One reason for this, as the model indicates, is due to the fact that Δv_{fi}° may be negative, while Δh_{fi}° is always positive. Liquid bismuth and antimony, which are unique metals since they have negative volume changes on fusion, are involved in mixtures that often have excess volumes, which differ in sign from corresponding excess enthalpies and Gibbs energies. The model can predict this situation to some degree. Finally, the model indicates that asymmetry and $\Delta\beta_{fi}^\circ$ also play important roles in explaining phenomena such as sign, magnitude, and shape behavior.

Therefore, the GHV model has provided valuable new insight into the nature of excess properties without resorting to adjustable parameters as yet. In the next section, however, the fusion properties are correlated to evaluate the quantitative

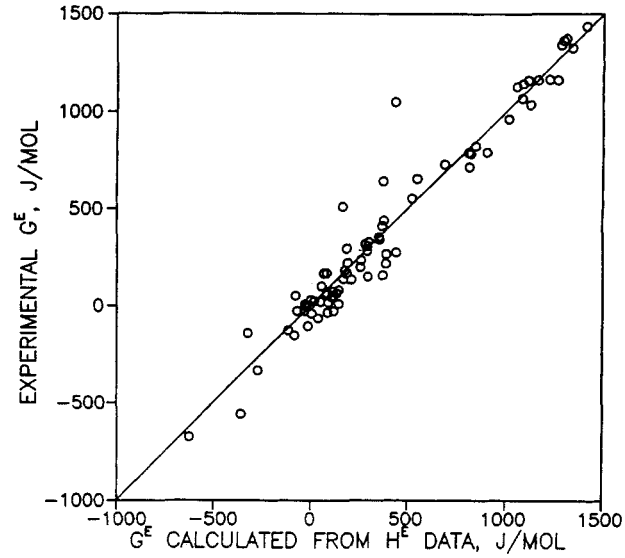

Figure 5. Equimolar excess Gibbs energies for organic mixtures at 25°C calculated from excess enthalpy data using effective fusion properties.

potential of the model and to better understand the fusion properties, for which reliable literatures values are unavailable.

Effective Fusion Properties

The test of the GHV model presented in the last section was rough since the model was applied under circumstances, for which it was not derived and uncertainties in the fusion properties prevented an adequate comparison between experimental and predicted values. To ameliorate these limitations, "effective" fusion properties were determined for the organic species at 25°C. This was done to further evaluate the quantitative potential and general applicability of the model. Only Δv_{EFF}, Δh_{EFF}, $\Delta C_{P,EFF}$, and $\Delta\beta_{EFF}$ were found, while $\Delta_f(\partial\bar{h}_i^E/\partial T)_{x,P}^\infty$ and $\Delta_f(\partial\bar{v}_i^E/\partial P)_{x,P}^\infty$ were still ignored in the model equations. These effective parameters were determined by fitting the GHV equations to equimolar excess Gibbs energy data, and each compound in the database was involved in at least four mixtures, and eight or nine mixtures on average. Note that the same effective parameters were used for a particular compound regardless of the mixture. Liquid metal solutions will no longer be considered, since the data are very limited, often with poor quality, and determined at temperatures that vary greatly.

The resulting effective parameters are presented in Table 1, and the excess properties calculated from them are compared to experimental data in Table 2 and Figures 5 through 7. The effective parameters are generally of the proper magnitude, though some species (particularly ethanol) appear to exhibit problems. The magnitudes for ΔC_{Pfi}° compare well with some literature values that are available (Domalski et al., 1984) and reflect the fact that they can take on both positive and negative values. The magnitudes of the $\Delta\beta_{fi}^\circ$ are also quite reasonable, since they are on the order of one fourth of the organic liquid-phase compressibilities (Weast and Astle, 1980) and should almost always be negative.

Although the solutions vary greatly, and each species was involved in a number of mixtures, the excess Gibbs energy

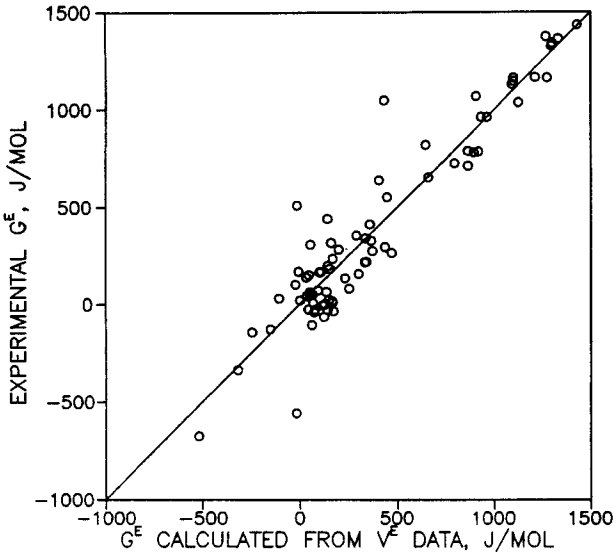

Figure 6. Equimolar excess Gibbs energies for organic mixtures at 25°C calculated from excess volume data using effective fusion properties.

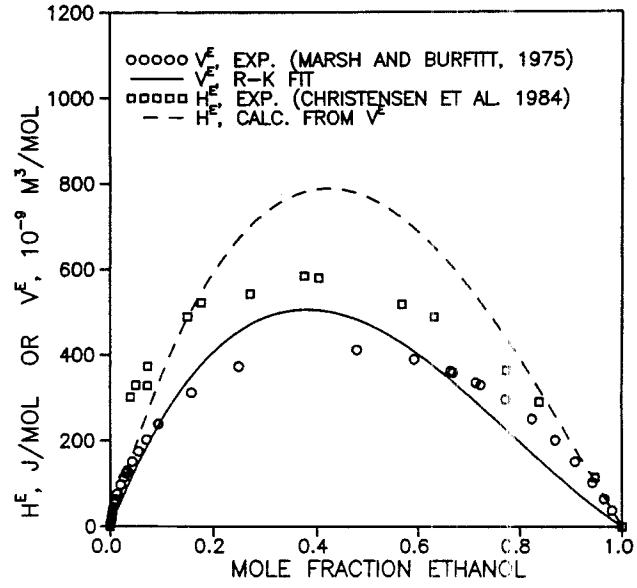

Figure 8. Comparison between excess enthalpies determined experimentally and calculated from excess volumes using effective fusion properties for ethanol/*n*-hexane mixtures.

values calculated from excess volume and enthalpy data are reasonably quantitative. The excess enthalpies, calculated from excess volume data (in Figure 7), show more scatter since this combination was fit in only an indirect manner. These results lend credence to the GHV model's premise that certain pure component properties exist which can be used to interrelate excess properties, no matter what mixtures they may be involved in.

The model also does a reasonably good job of predicting the relative shapes of the excess property curves, even though only equimolar excess Gibbs energies were used in the correlation. For example, Figure 8 illustrates the rather asymmetric excess volumes for the ethanol/*n*-hexane system. The excess enthalpies calculated from these asymmetric excess volume data (in Figure 8) agree well with the experimental results, both in magnitude and shape (which is slightly less asymmetric). The excess Gibbs energies for this mixture in Figure 9 show good magnitude and shape agreement between the calculated and experimental results. Note that the excess volumes are more asymmetric than the excess enthalpies, which in turn are more asymmetric than the excess Gibbs energies. This is a very

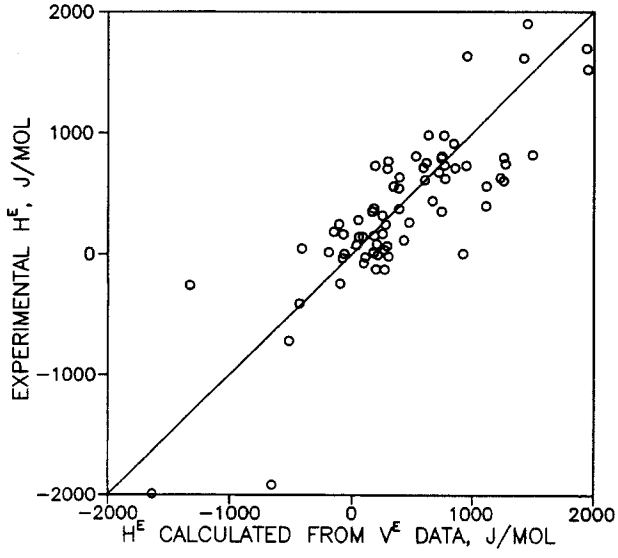

Figure 7. Equimolar excess enthalpies for organic mixtures at 25°C calculated from excess volume data using effective fusion properties.

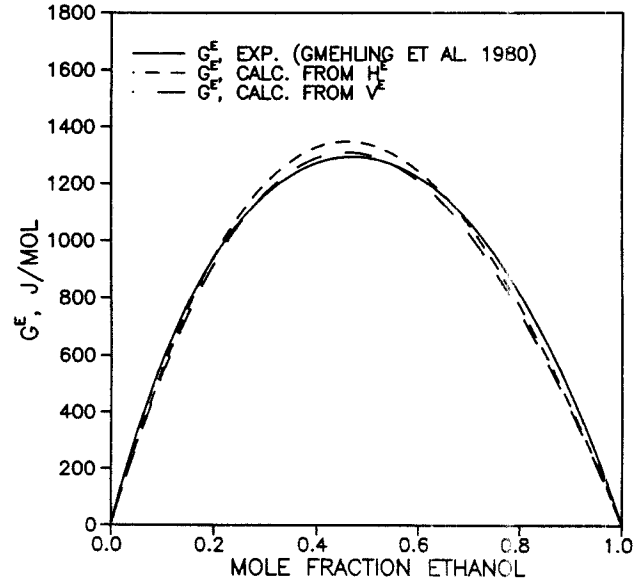

Figure 9. Comparison between excess Gibbs energies determined experimentally and calculated from excess volumes and enthalpies using effective fusion properties for ethanol/*n*-hexane mixtures.

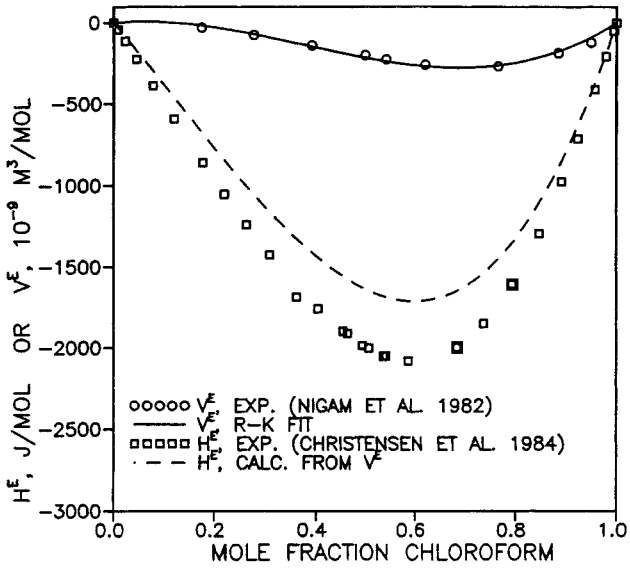

Figure 10. Comparison between excess enthalpies determined experimentally and calculated from excess volumes using effective fusion properties for chloroform/1,4 dioxane mixtures.

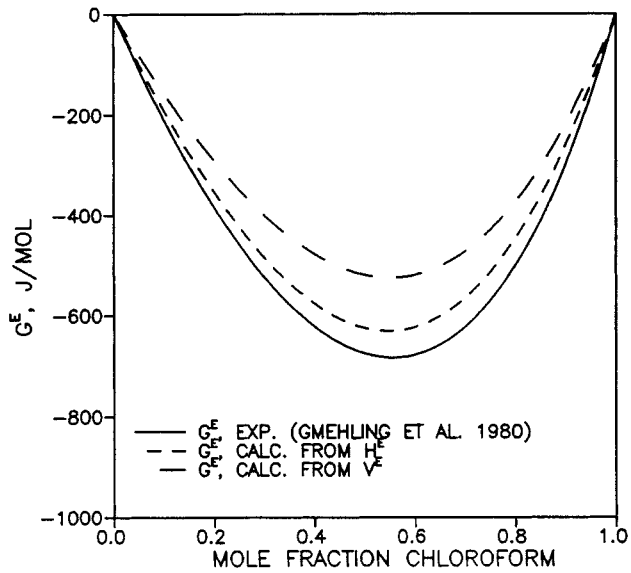

Figure 11. Comparison between excess Gibbs energies determined experimentally and calculated from excess volumes and enthalpies using effective fusion properties for chloroform/1,4 dioxane mixtures.

common trend, and the GHV model does an excellent job of predicting this situation.

An even more extreme example of the model's ability to predict shape phenomena is shown in Figures 10 and 11 for the chloroform/1,4 dioxane systems. These solutions actually have small, highly asymmetric, 'S'-shaped excess volumes. The model, however, still predicts the proper magnitudes and shapes for the excess Gibbs energies and enthalpies calculated from them. The trend noted above has again been observed and predicted. The ability of the GHV model to predict shape characteristics of the excess properties is of much interest since the determination of some derivative phenomena such as liquid-liquid immiscibility depends strongly on composition dependencies (Trampe, 1989).

Conclusions

Even though trends and similarities between the excess thermodynamic properties have long been recognized, current solution models are generally incapable of cross-predicting them (Trampe, 1989). The GHV model developed here, which interrelates excess Gibbs energies, enthalpies, and volumes, should be useful in alleviating this inconsistency. The model was derived in a fairly rigorous, fundamental manner, utilizing the single assumption that the mixture is immiscible in solid phases, and, therefore, has wide applicability. The model was applied to both diverse organic and metallic solutions and provided invaluable insight into the factors that affect relative sign, magnitude and shape phenomena. However, the results obtained here are somewhat preliminary and further work is necessary, in particular:

- To apply model to other mixtures, including electrolytic and polymeric solutions, and to evaluate further the acceptable ranges of solid solubilities
- To improve temperature extrapolation of model equations
- To determine more appropriate excess property functionality
- To measure more fusion properties, especially Δv_f^* and $\Delta\beta_f^*$
- To use model equations to evaluate solid-phase partial molar excess volumes and enthalpies.

Acknowledgment

The authors are grateful to the Standard Oil Co. (Indiana), the E. I. DuPont de Nemours Co., and the Link Foundation for their financial support.

Notation

A_θ, B_θ = Redlich-Kister parameters for excess properties
ΔC_{Pfi}^* = pure component molar heat capacity change on fusion
g = molar Gibbs free energy
h = molar enthalpy
Δh_{fi}^* = pure component molar enthalpy of fusion of i
P = pressure
SLE = solid-liquid equilibrium
T = temperature
v = molar volume
Δv_{fi}^* = pure component molar volume change on fusion of i
x = composition, mole fraction

Greek letters

$\Delta\beta_{fi}^*$ = pure component change of $(\partial v_i/\partial P)_T$ on fusion of i
γ = activity coefficient
μ = chemical potential

Superscripts

E = excess property
L = liquid-phase property
S = solid-phase property
$-$ = partial molar property
∞ = infinite dilution property

Subscripts

EFF = correlated, effective fusion property
i = general index referring to any component
M = melting point property
1 = property of component 1
2 = property of component 2

Literature Cited

Babb, S. E., "Parameters in the Simon Equation Relating Pressure and Melting Temperature," *Rev. Mod. Phys.*, **35**, 400 (1963).

Christensen, C., J. Gmehling, P. Rasmussen, and U. Weidlich, *Heats of Mixing Data Collection*, Dechema, Frankfurt (1984).

Denbigh, K., *The Principles of Chemical Equilibrium*, 4th ed., Cambridge University Press, London (1981).

Domalski, E. S., W. H. Evans, and E. D. Hearing, "Heat Capacities and Entropies of Organic Compounds in the Condensed Phase," *J. Phys. Chem. Ref. Data*, **13**, 1 (1984).

Gmehling, J., U. Onken, and W. Arlt, *Vapor-Liquid Equilibrium Data Collection*, Dechema, Frankfurt (1980).

Goates, J. R., J. B. Ott, and R. B. Grigg, Excess Volumes of *n*-Hexane + *n*-Heptane, + *n*-Octane, + *n*-Nonane, and + *n*-Decane at 283.15, 298.15 and 313.15 K," *J. Chem. Thermody.*, **13**, 907 (1981).

Hamann, S. D., *Physico-Chemical Effects of Pressure*, Academic Press, New York (1957).

Handa, Y. P., G. C. Benson, "Volume Changes on Mixing Two Liquids: a Review of the Experimental Techniques and the Literature Data," *Fluid Phase Equilib.*, **3**, 185 (1979).

Hansen, A. R., and C. A. Eckert, "A Relationship between Excess Volumes and Enthalpies," *Fluid Phase Equil.*, accepted (1990).

Hansen, A. R., M. A. Kaminski, C. T. Lira, and C. A. Eckert, "Volumes and Excess Volumes of Some Liquid Metals and Alloys," *Ind. Eng. Chem. Res.*, **28**, 97 (1989).

Hansen, A. R., M. A. Kaminski, and C. A. Eckert, "Molar and Excess Volumes of Liquid In-Sb, Mg-Sb, and Pb-Sb Alloys," *J. Chem. Eng. Data*, **35**, 153 (1990).

Lepori, L., and E. Matteoli, "Excess Volumes of (Tetrachloromethane + an Alkanol or + a Cyclic Ether) at 298.15 K," *J. Chem. Thermody.*, **18**, 13 (1986).

Lira, C. T., "Volumetric Behavior of Liquid Metal and Alloys," PhD Thesis, Univ. of Illinois, Urbana (1986).

Marsh, K. N., and C. Burfitt, "Excess Volumes for Alcohols + Nonpolar Solvents: I. Ethanol + Cyclohexane, + *n*-Hexane, + Benzene, + Carbon Tetrachloride, + Cyclopentane, and + *p*-Xylene," *J. Chem. Thermody.*, **7**, 955 (1975).

Nigam, R. K., B. S. Mahl, and P. P. Singh, "Excess Volumes of Mixing," *J. Chem. Thermody.*, **4**, 41 (1972).

Prausnitz, J. M., R. N. Lichtenthaler, and E. G. de Azevedo, *Molecular Thermodynamics of Fluid-Phase Equilibria*, 2nd ed., Prentice Hall, Englewood Cliffs, NJ (1986).

Rodriguez-Nunez, E., M. I. Paz-Andrade, and R. Bravo, "Thermodynamic Properties of (a Xylene + an *n*-Alkanol): III. Excess Molar Volumes at 298.15 K for 1-Hexanol, 1-Heptanol, and 1-Octanol," *J. Chem. Thermody.*, **17**, 817 (1985).

Trampe, D. M., "Measurement, Prediction, and Application of the Limiting Activity Coefficient and Its Temperature Derivative," PhD Thesis, Univ. of Illinois, Urbana (1989).

Treszczanowicz, A. J., and G. C. Benson, "Excess Volumes for *n*-Alkanols + *n*-Alkanes: I. Binary Mixtures of Methanol, Ethanol, *n*-Propanol, and *n*-Butanol + *n*-Heptane," *J. Chem. Thermody.*, **9**, 1189 (1977).

Weast, R. C., and M. J. Astle, eds., *CRC Handbook of Chemistry and Physics*, 61st ed., CRC Press, Boca Raton, FL (1980).

Manuscript received June 28, 1990, and revision received Oct. 30, 1990.